IEEE Photonics Journal
An IEEE Photonics Society Publication

Open Access

Experimentally Validated Dispersion Tailoring in a Silicon Strip Waveguide With Alumina Thin-Film Coating

Volume 10, Number 2, April 2018

Kai Guo
Jesper. B. Christensen
Xiaodong Shi
Erik. N. Christensen
Li Lin
Yunhong Ding
Haiyan Ou
Karsten Rottwitt

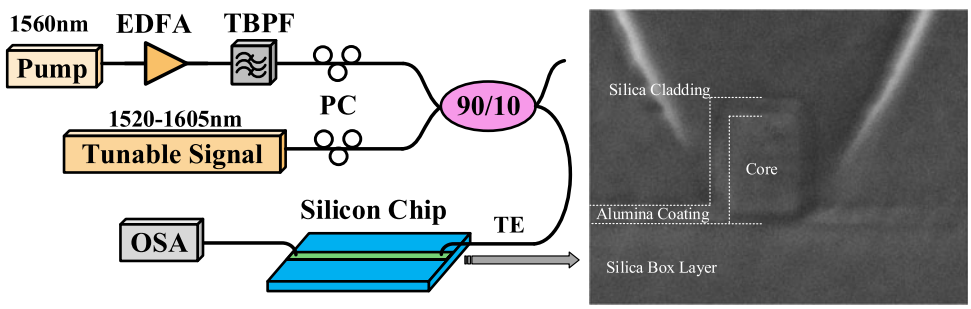

DOI: 10.1109/JPHOT.2018.2802931
1943-0655 © 2018 IEEE

IEEE photonics SOCIETY

IEEE

Experimentally Validated Dispersion Tailoring in a Silicon Strip Waveguide With Alumina Thin-Film Coating

Kai Guo, Jesper. B. Christensen, Xiaodong Shi, Erik. N. Christensen, Li Lin, Yunhong Ding, Haiyan Ou, and Karsten Rottwitt

College of Optoelectronic Science and Engineering, National University of Defense Technology, Changsha 410073 China, and the Department of Photonics Engineering, Technical University of Denmark, Lyngby 2800, Denmark

DOI:10.1109/JPHOT.2018.2802931

Manuscript received December 20, 2017; revised January 22, 2018; accepted February 2, 2018. Date of publication February 6, 2018; date of current version February 19, 2018. This work was supported in part by the Chinese Scholarship Council, in part by the Natural Science Foundation of China under Grants 61465015 and 60907003, in part by the Foundation of NUDT under Grant JC13-02-13, in part by the Hunan Provincial Natural Science Foundation of China under Grant 13JJ3001, in part by the Program for New Century Excellent Talents in University (NCET-12-0142), and in part by the Danish National Research Foundation (DNRF123). Corresponding author: Kai Guo (e-mail: guokai07203@nudt.edu.cn).

Abstract: We propose a silicon strip waveguide structure with alumina thin-film coating in-between the core and the cladding for group-velocity dispersion tailoring. By carefully designing the core dimension and the coating thickness, a spectrally-flattened near-zero anomalous group-velocity dispersion within the telecom spectral range is obtained, which is predicted to significantly broaden the bandwidth of four-wave mixing. We validate this by characterizing the wavelength conversion in a waveguide sample by atomic layer deposition technology, which to our best knowledge is the first experimental demonstration of the proposed structure. Due to the alumina thin-film coating, the wavelength conversion bandwidth reaches 58 nm, an increase by a factor of 1.3 compared to the corresponding structure without coating. This method can also be applied to other material platforms and applications requiring accurate group-velocity dispersion control.

Index Terms: Silicon nanophotonics, waveguide devices, thin film coatings, four-wave mixing.

1. Introduction

Wavelength conversion based on four-wave mixing (FWM), which has been achieved in highly nonlinear fibers [1] and on-chip waveguide platforms [2], [3], is of great significance in a number of applications such as wavelength division multiplexing networks [4]. In the past decade, silicon waveguides have attracted interest in optical communication research, due to their fabrication compatibility with the complementary metal oxide semiconductor (CMOS) technology [5], which enables easy integration of various electrically or optically driven components, including optical modulators [6], power splitters [7], polarizers [8], and optical filters [9], [10]. Moreover, silicon waveguides have high refractive index contrast relative to silica, which enables high-density integrated lightwave circuitry and efficient nonlinear interaction. The group-velocity dispersion (GVD) is a key parameter

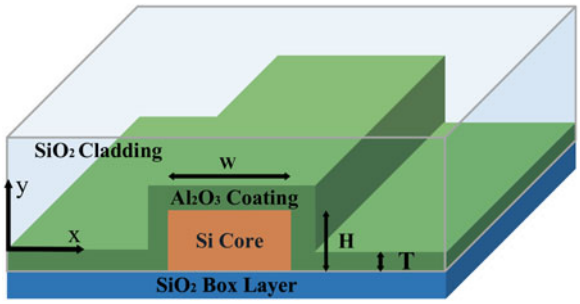

Fig. 1. The proposed structure including a silicon core, height of H and width of W, an alumina thin-film coating, thickness of T, and a silica cladding.

for the FWM process that can be tailored via flexible geometry design of silicon waveguides. Hence, broadband wavelength conversion [11], [12] and multicasting [13], [14] have been demonstrated in GVD-tailored silicon waveguides.

A number of wavelength conversion experiments have been carried out based on degenerate FWM, in which two pump photons with the same frequency are annihilated and a pair of signal-idler photons are generated. Efficient and broadband FWM takes place when the pump experiences near-zero anomalous GVD [15]. By using the second-order derivative of the propagation constant with respect to the angular frequency, $\beta_2(\omega)$, near-zero and anomalous GVD are described as $\beta_2 \approx 0$ $\beta_2 < 0$, respectively, at the pump wavelength. Spectrally-flattened GVD ($d\beta_2/d\omega \approx 0$) is further desired in supercontinuum generation [16]. Previous GVD tailoring studies have mainly focused on the geometry design of the silicon core. In the common structure where the core is rectangular shaped [12], [17], the height H is determined by the thickness of the silicon layer in a silicon-on-insulator (SOI) wafer, and thus the width W is the only degree of freedom which can be varied freely to tailor spectrally-flattened near-zero anomalous GVD.

Here, we propose a structure with an alumina thin-film coating [18] and a silica cladding (see Fig. 1). Based on the atomic layer deposition (ALD) technology [19], [20], the coating thickness T can be accurately controlled so that an extra degree of freedom for GVD tailoring is added. Therefore, GVD tailoring using T as the main degree of freedom benefits from high fabrication accuracy, and small GVD variations from sample to sample. Moreover, the refractive index of the thin-film coating can be introduced as another degree of freedom, which provides a variety of materials to choose. Note that the proposed structure uses alumina instead of titania employed in [21], due to its relatively lower loss in the telecom spectral range (1460 nm–1625 nm). Hence, the proposed structure can be, under similar strategy, used to tailor GVD that is easily validated by experiments. The concept of using thin-film coating for the proposed structure is also different from that shown in [16] and [22], in which thin-film coatings, sandwiched in silicon layers, are used to guide the "slot-modes". As we carefully design the geometry of the waveguide so that the optical field is mainly confined in the silicon region corresponding to highly nonlinear interaction [23], the proposed structure holds potential to achieve high efficiency and broad bandwidth of wavelength conversion, simultaneously.

In this paper, we demonstrate how an alumina-coated SOI waveguide can be used to achieve spectrally-flattened near-zero anomalous GVD in the telecom spectral range. We perform a proof-of-concept experiment, and achieve good agreement between numerical simulations and experimental measurements, which becomes the first explicit validation of the proposed structure for broadband wavelength conversion. The resulting wavelength conversion bandwidth is 30% broader than that achievable with the corresponding non-coated structure, and the bandwidth can be further broadened by employing thicker alumina coatings.

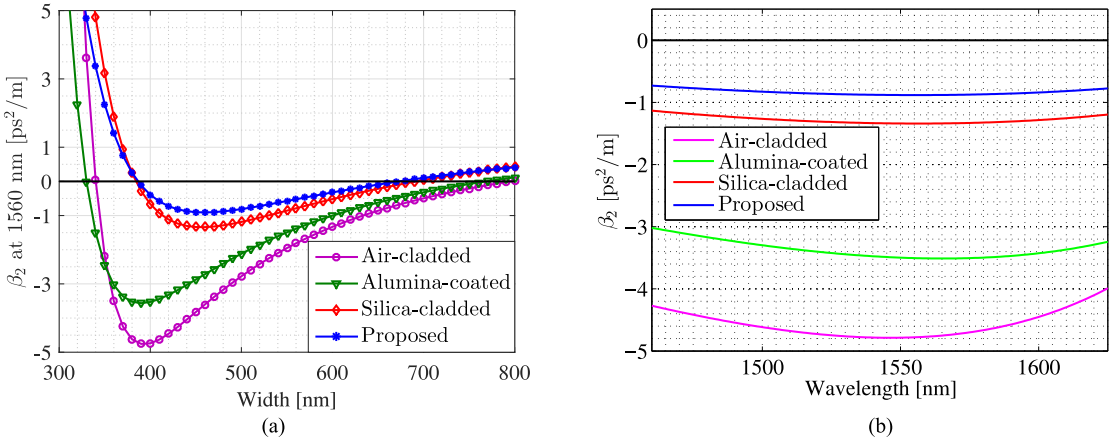

Fig. 2. (a) β_2 at 1560 nm versus core width W for the air-cladded structure (magenta circles), the alumina-coated structure (green triangles), the silica-cladded structure (red diamonds), and the proposed structure (blue asterisks). (b) β_2 versus wavelength for the air-cladded structure (magenta), the alumina-coated structure (green) when $W = 390$ nm, and for the silica-cladded structure (red), the proposed structure (blue) when $W = 460$ nm.

2. Numerical Results

2.1 Group-Velocity Dispersion Tailoring

We have used a finite-difference mode solver [24] to simulate the field profiles of waveguides with core heights (H) of 250 nm. Fig. 2(a) shows β_2 versus core width (W) at 1560 nm in the fundamental transverse electric (TE_{01}) mode, for the air-cladded structure, the silica-cladded structure, the alumina-coated (and air-cladded) structure, and the proposed structure (with both thin-film coating and silica cladding), respectively, where the initial coating thickness is 50 nm. The wavelength dependent refractive index of the thin-film alumina is considered in numerical simulations, of which the data comes from [18]. For the air-cladded structure, one gets anomalous GVD using a core width in-between 340 nm and 790 nm. When the core width is wider than 700 nm, $|\beta_2|$ becomes near-zero, but the large mode area consequently reduces the field intensity and further weakens the nonlinear interaction [12]. A core width of 340 nm results in a near-zero anomalous GVD ($\beta_2 = -0.04\,\text{ps}^2/\text{m}$) and a small mode area at 1560 nm, but the core width deviation in fabrication process can cause a huge variation on the GVD. Such a variation is mitigated for the alumina-coated structure, the silica-cladded structure and especially the proposed structure.

By using the core width that corresponds to a zero slope of β_2 in Fig. 2(a), GVD is stable in terms of fabrication accuracy. Such a core width also enables spectrally-flattened GVD, but the absolute value $|\beta_2|$ reaches the maximum. Fig. 2(b) shows that for the air-cladded structure ($W = 390$ nm), $|\beta_2|$ is larger than $4\,\text{ps}^2/\text{m}$ for all considered wavelengths. The maximal $|\beta_2|$ reduces to $3.4\,\text{ps}^2/\text{m}$ and $1.3\,\text{ps}^2/\text{m}$ for the alumina-coated structure ($W = 390$ nm) and for the silica-cladded structure ($W = 460$ nm), respectively. A maximal $|\beta_2|$ of $0.9\,\text{ps}^2/\text{m}$ is obtained for the proposed structure ($W = 460$ nm). Furthermore, by increasing the coating thickness T, the value of $|\beta_2|$ can be made even smaller. Fig. 3(a) shows how the GVD is gradually shifted towards the normal GVD region as the coating thickness increases. The maximal value of $|\beta_2|$ are $0.54\,\text{ps}^2/\text{m}$ ($T = 100$ nm, $W = 470$ nm), $0.30\,\text{ps}^2/\text{m}$ ($T = 150$ nm, $W = 480$ nm), $0.17\,\text{ps}^2/\text{m}$ ($T = 200$ nm, $W = 490$ nm), and $0.09\,\text{ps}^2/\text{m}$ ($T = 250$ nm, $W = 510$ nm), respectively. At this point, GVD remains spectrally-flattened, and becomes near-zero (see Fig. 3(b)). Additionally, as the impact of the coating thickness becomes significant when a core width corresponding to the zero slope of β_2 is employed, accurate GVD control can be achieved by precisely controlling the coating deposition.

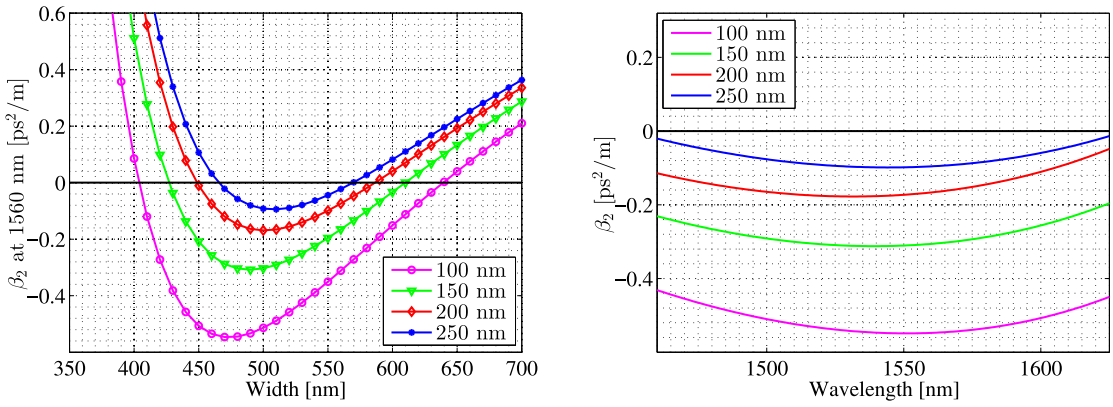

Fig. 3. (a) β_2 at 1560 nm versus W in the proposed structure for different coating thickness T of 100 nm (magenta circles),150 nm (green triangles), 200 nm (red diamonds), and 250 nm (blue asterisks). (b) β_2 versus wavelength in the proposed structure when $T = 100$ nm and $W = 470$ nm (magenta), $T = 150$ nm and $W = 480$ nm (green), $T = 200$ nm and $W = 490$ nm (red),$T = 250$ nm and $W = 510$ nm (blue).

2.2 Modeling of Wavelength Conversion

The common method to evaluate GVD is to characterize the 3 dB bandwidth of the wavelength conversion efficiency, which is given by the ratio of the idler power to the signal power, $\eta = \mathrm{P_i(L)/P_s(L)}$, at the output of the waveguide of length L , and can be obtained by solving [25]

$$\frac{dA_p}{dz} = -\frac{1}{2}\alpha_p A_p + i\gamma_e |A_p|^2 A_p \,, \tag{1}$$

$$\frac{dA_s}{dz} = -\frac{1}{2}\alpha_s A_s + 2i\gamma_e |A_p|^2 A_s + i\gamma_e A_p^2 A_i^* e^{-i\Delta\beta z} \,, \tag{2}$$

$$\frac{dA_i}{dz} = -\frac{1}{2}\alpha_i A_i + 2i\gamma_e |A_p|^2 A_i + i\gamma_e A_p^2 A_s^* e^{-i\Delta\beta z} \,, \tag{3}$$

where $A_j (j = p, s, i)$ denote the normalized amplitude of the pump, signal and idler, respectively, and $|A_j|^2$ equals the optical power P_j. The complex nonlinear coefficient γ_e consists of a real part representing Kerr effect and an imaginary part representing two-photon absorption (TPA)

$$\gamma_e = \frac{\zeta_e \omega_j n_2}{c A_{\mathrm{eff}}} + \frac{i\zeta_e \beta_T}{2A_{\mathrm{eff}}} \,. \tag{4}$$

In (4), where only the contribution of silicon is considered, the intensity-dependent refractive index n_2 is $6 \cdot 10^{-18}$ m^2/W, the TPA coefficient β_T is $4.5 \cdot 10^{-12}$ m/W, the polarization coefficient ζ_e is 1.25 for TE mode [23], [26], and the effective mode area A_{eff} is calculated through a full-vectorial model [25]. Moreover, the loss coefficient α_j in (1)–(3) includes the wavelength-independent linear loss α_l and the wavelength-dependent free carrier absorption (FCA) [27]

$$\alpha_{f,j} = 6.04 \times 10^{-10} \lambda_j^2 \frac{\zeta_e \beta_T |A_p|^4 \tau}{2\hbar\omega_p A_{\mathrm{eff}}^2} \,, \tag{5}$$

where τ is the free carrier lifetime that is set as 10 ns. Additionally, the linear phase mismatch $\Delta\beta$ is obtained from the GVD at pump and the signal-pump detuning.

Fig. 4(a) shows A_{eff} versus wavelength ($W = 460$ nm) for the proposed structures, which becomes larger with increasing coating thickness. The proposed structure has an approximate A_{eff} to the corresponding silica-cladded structure. The inset of Fig. 4(a) shows the squared x-component of the electric field for the proposed structure with a coating thickness of 50 nm, indicating that the optical field is dominantly confined in the silicon core. Such a structure makes possible

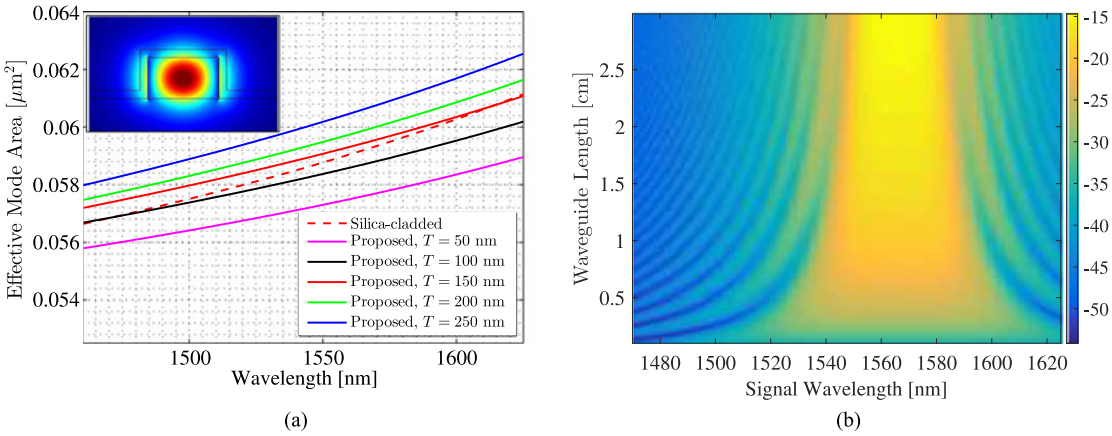

Fig. 4. (a) Effective mode area A_{eff} versus wavelength for the silica-cladded structure (red dashed), and the proposed structures with T of 50 nm (magenta solid), 100 nm (black solid),150 nm (red solid), 200 nm (green solid) and 250 nm (blue solid). The inset is the field distribution at 1560 nm when $T = 50$ nm for the proposed structure. (b) Conversion efficiency η versus signal wavelength and waveguide length. The pump is at 1560 nm, with a power of 15 dBm. The signal power is -10 dBm. The core width is 460 nm.

high-efficiency broadband wavelength conversion. We then based on this structure numerically calculate conversion efficiency versus signal wavelength and waveguide length by solving (1)–(3), setting the power of pump and signal as 15 dBm and -10 dBm, respectively. The parameters used in the calculation are set so as to best comply with those used in the experiment (see Section 3). Fig. 4(b) shows that the maximal conversion efficiency with respect to the signal wavelength, for the proposed structure with coating thickness of 50 nm, increases as the waveguide length increases until 2 cm, and then slowly saturates. Meanwhile, the 3 dB bandwidth becomes increasingly narrow as the waveguide length increases. Although a long waveguide facilitates high conversion efficiency, it suffers from a narrow bandwidth. Compared with the silica-cladded structure, of which the 3 dB bandwidth is 36 nm at 1 cm [25], the proposed structure broadens the bandwidth by a factor of 1.3 to 48 nm. As the nonlinear coefficient remains almost unchanged, such a bandwidth broadening can be mainly attributed to the efficient dispersion tailoring. A further bandwidth improvement can be obtained by using a larger coating thickness. For example, by using a 250 nm coating thickness, the 3 dB bandwidth at a waveguide length of 1 cm is 96 nm corresponding to a factor of 2.7 improvement compared to the silica-cladded structure.

3. Waveguide Fabrication and Wavelength Conversion Measurement

To verify GVD tailoring and numerical predictions of the wavelength conversion, we fabricated a waveguide sample. First, a standard SOI nano-fabrication process, including e-beam lithography and inductively coupled plasma (ICP) etching, was used to fabricate the fully etched photonic crystal based grating couplers (PCGCs) [28], [29] and the silicon strip waveguide simultaneously. For quick fabrication and experimental validation, a 50 nm-thick alumina coating was deposited by ALD system, and a 1 μm-thick silica cladding was deposited by the plasma enhanced chemical vapor deposition. A 50 nm-thick alumina coating was deposited by ALD system, and a 1 μm-thick silica cladding was deposited by the plasma enhanced chemical vapor deposition. A cross-sectional Scanning Electron Microscope (SEM) image of a test (not the investigated) sample is shown in Fig. 5.

As shown in the schematic experimental setup, a pump at 1560 nm was amplified by an erbium-doped fiber amplifier (EDFA), and the amplified spontaneous emission was filtered by a tunable band-pass filter (TBPF). A tunable laser with a tuning range of 1520 nm–1605 nm was used as

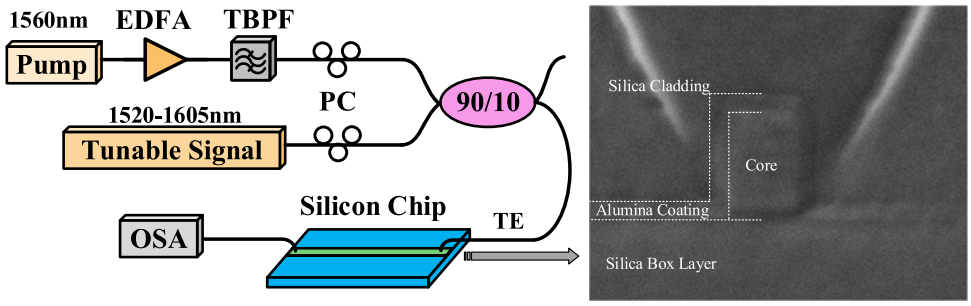

Fig. 5. Experimental setup of FWM wavelength conversion using a 6 mm sample. The component abbreviations are: EDFA: erbium-doped fiber amplifier, TBPF: tunable band-pass filter, PC: polarization controller, OSA: optical spectrum analyser. The inset is the cross-sectional SEM image of a test (not the investigated) sample, from which we can distinguish the silica box layer, the silicon core, the alumina thin-film coating and the silica cladding.

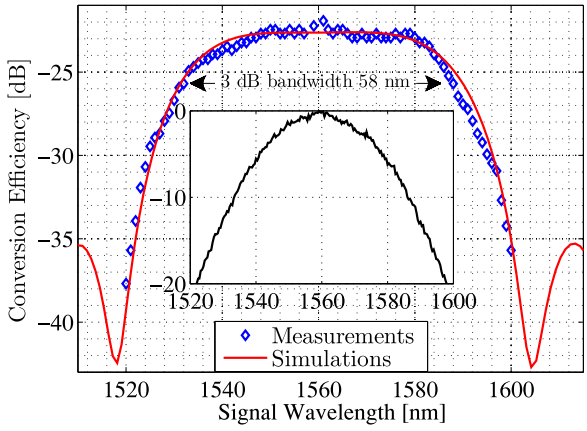

Fig. 6. Experimental measurements (blue diamond) and numerical predictions (red solid) of conversion efficiency versus wavelength. The inset illustrates the normalized transmittance of PCGCs measured by a supercontinuum laser.

signal. The pump and the signal were combined by a 90%–10% coupler, and their polarizations were independently controlled by polarization controllers (PCs). A pair of PCGCs, designed for the silica-cladded structure [29] but remained valid for the proposed structure, were employed, of which the total normalized transmittance, measured by a supercontinuum laser, was shown in Fig. 6 inset. The light was vertically coupled in and out of the proposed chip at 20° (commonly 10° for the silica-cladded chips), with the normalized transmittance of PCGCs centered at 1560 nm and a 3 dB bandwidth of 28 nm. The minimal alignment loss was 10 dB, and the propagation loss was estimated to 3 dB/cm. The idler power at the end of the 6 mm waveguide sample was estimated by subtracting the normalized transmittance of output PCGC from the data measured by an optical spectrum analyzer (OSA), and was further modified by taking the in-waveguide incident signal power, being wavelength-dependent induced by input PCGC with a highest value of −10 dBm at 1560 nm, into account. Since the signal power at the end of the investigated waveguide was also modified using the normalized transmittance of output PCGC, and the in-waveguide incident pump power was estimated at 15 dBm, the resulting modified conversion efficiency was carried out under the same condition with numerical simulations.

In Fig. 6, we show the experimental measurements and the numerical simulations simultaneously. The maximal modified conversion efficiency is −22 dB, with a 3 dB bandwidth of 58 nm, which agrees well with the simulation. Note that we use free-carrier lifetime as a fitting parameter, and

the value of 10 ns, enabling a good agreement between simulations and measurements, is also used to the numerical prediction in Section 2. Moreover, by using the same simulation model and parameters, we simulate the conversion efficiency for a silicon waveguide with only silica cladding, and a 3 dB bandwidth of 42 nm is obtained. Thus, introducing the 50 nm-thick thin-film coating makes possible a 1.3 times broader 3 dB bandwidth. In future work, the 3 dB bandwidth of the conversion efficiency can be further broadened by using a thicker alumina coating. In addition, other materials, which have high transmittance and suitable refractive index, could be selected as the thin-film coating between silicon core and silica cladding, preferable to be compatible with the atomic layer deposition technology, so that accurate GVD control is accessible. The proposed structure can be also applied to other on-chip platforms.

4. Conclusion

In conclusion, we show that the proposed structure, employing alumina thin-film coating in-between the silicon core and the silica cladding, achieves spectrally-flattened near-zero anomalous group-velocity dispersion. We demonstrate group-velocity dispersion tailoring by optimizing the waveguide geometry, and numerically predict the efficiency of wavelength conversion. We fabricated a sample and characterized the four-wave mixing as an explicit verification of our numerical predictions, and achieve a 3 dB bandwidth of 58 nm. The experimental demonstration is, to our best knowledge, the first proof of the proposed structure valid to tailor GVD. Additionally, the proposed waveguide structure can be adopted to other on-chip platforms, and is useful not only for broadband wavelength conversion applications, but whenever accurate group-velocity dispersion control is required.

Acknowledgment

The authors would also like to thank Xiaowei Guan, Junbo Yang, Minghong Gao and Jiehui Li for useful discussions.

References

[1] J. H. Lee *et al.*, "Four-wave mixing based 10-gb/s tunable wavelength conversion using a holey fiber with a high SBS threshold," *IEEE Photon. Technol. Lett.*, vol. 15, no. 3, pp. 440–442, Mar. 2003.
[2] M. A. Foster, A. C. Turner, J. E. Sharping, B. S. Schmidt, M. Lipson, and A. L. Gaeta, "Broad-band optical parametric gain on a silicon photonic chip," *Nature*, vol. 441, no. 7096, pp. 960–963, 2006.
[3] P. Apiratikul *et al.*, "Enhanced continuous-wave four-wave mixing efficiency in nonlinear AlGaAs waveguides," *Opt. Exp.*, vol. 22, no. 22, pp. 26 814–26 824, 2014.
[4] S. B. Yoo, "Wavelength conversion technologies for WDM network applications," *J. Lightw. Technol.*, vol. 14, no. 6, pp. 955–966, Jun. 1996.
[5] P. Dong, Y.-K. Chen, G.-H. Duan, and D. T. Neilson, "Silicon photonic devices and integrated circuits," *Nanophotonics*, vol. 3, no. 4–5, pp. 215–228, 2014.
[6] L. O'Faolain, D. M. Beggs, T. P. White, T. Kampfrath, K. Kuipers, and T. F. Krauss, "Compact optical switches and modulators based on dispersion engineered photonic crystals," *IEEE Photon. J.*, vol. 2, no. 3, pp. 404–414, Jun. 2010.
[7] Y. Wang, S. Gao, K. Wang, and E. Skafidas, "Ultra-broadband and low-loss 3 dB optical power splitter based on adiabatic tapered silicon waveguides," *Opt. Lett.*, vol. 41, no. 9, pp. 2053–2056, 2016.
[8] Q. Wang and S.-T. Ho, "Ultracompact TM-pass silicon nanophotonic waveguide polarizer and design," *IEEE Photon. J.*, vol. 2, no. 1, pp. 49–56, Feb. 2010.
[9] R. Halir *et al.*, "Recent advances in silicon waveguide devices using sub-wavelength gratings," *IEEE J. Sel. Topics Quantum Electron.*, vol. 20, no. 4, pp. 279–291, Jul./Aug. 2014.
[10] W. Bogaerts *et al.*, "Silicon-on-insulator spectral filters fabricated with CMOS technology," *IEEE J. Sel. Topics Quantum Electronics*, vol. 16, no. 1, pp. 33–44, Jan./Feb. 2010.
[11] H. Hu *et al.*, "Ultra-high-speed wavelength conversion in a silicon photonic chip," *Opt. Exp.*, vol. 19, no. 21, pp. 19 886–19 894, 2011.
[12] Y. Ding, J. Xu, H. Ou, and C. Peucheret, "Mode-selective wavelength conversion based on four-wave mixing in a multimode silicon waveguide," *Opt. Exp.*, vol. 22, no. 1, pp. 127–135, 2014.
[13] M. Pu *et al.*, "One-to-six WDM multicasting of DPSK signals based on dual-pump four-wave mixing in a silicon waveguide," *Opt. Exp.*, vol. 19, no. 24, pp. 24 448–24 453, 2011.
[14] M. Chagnon, M. Spasojevic, R. Adams, J. Li, D. V. Plant, and L. R. Chen, "Wavelength multicasting at 22-gbaud 16-QAM in a silicon nanowire using four-wave mixing," *IEEE Photon. Technol. Lett*, vol. 27, no. 8, pp. 860–863, Apr. 2015.

[15] J. Hansryd, P. A. Andrekson, M. Westlund, J. Li, and P.-O. Hedekvist, "Fiber-based optical parametric amplifiers and their applications," *IEEE J. Sel. Topics Quantum Electron.*, vol. 8, no. 3, pp. 506–520, May/Jun. 2002.
[16] L. Zhang, Q. Lin, Y. Yue, Y. Yan, R. G. Beausoleil, and A. E. Willner, "Silicon waveguide with four zero-dispersion wavelengths and its application in on-chip octave-spanning supercontinuum generation," *Opt. Exp.*, vol. 20, no. 2, pp. 1685–1690, 2012.
[17] A. C. Turner *et al.*, "Tailored anomalous group-velocity dispersion in silicon channel waveguides," *Opt. Exp.*, vol. 14, no. 10, pp. 4357–4362, 2006.
[18] R. Boidin, T. Halenkovič, V. Nazabal, L. Beneš, and P. Němec, "Pulsed laser deposited alumina thin films," *Ceramics Int.*, vol. 42, no. 1, pp. 1177–1182, 2016.
[19] L. Karvonen *et al.*, "Low-loss multiple-slot waveguides fabricated by optical lithography and atomic layer deposition," *IEEE Photon. Technol. Lett.*, vol. 24, no. 22, pp. 2074–2076, Nov. 2012.
[20] M. Erdmanis *et al.*, "Towards broad-bandwidth polarization-independent nanostrip waveguide ring resonators," *Opt. Exp.*, vol. 21, no. 8, pp. 9974–9981, 2013.
[21] M. Erdmanis *et al.*, "ALD-assisted multiorder dispersion engineering of nanophotonic strip waveguides," *J. Lightw. Technol.*, vol. 30, no. 15, pp. 2488–2493, Aug. 2012.
[22] H. Liang, Y. He, R. Luo, and Q. Lin, "Ultra-broadband dispersion engineering of nanophotonic waveguides," *Opt. Exp.*, vol. 24, no. 26, pp. 29 444–29 451, 2016.
[23] H. Tsang *et al.*, "Optical dispersion, two-photon absorption and self-phase modulation in silicon waveguides at 1.5 μm wavelength," *Appl. Phys. Lett.*, vol. 80, no. 3, pp. 416–418, 2002.
[24] A. B. Fallahkhair, K. S. Li, and T. E. Murphy, "Vector finite difference modesolver for anisotropic dielectric waveguides," *J. Lightw. Technol.*, vol. 26, no. 11, pp. 1423–1431, Jun. 2008.
[25] K. Guo *et al.*, "Full-vectorial propagation model and modified effective mode area of four-wave mixing in straight waveguides," *Opt. Lett.*, vol. 42, no. 18, pp. 3670–3673, 2017.
[26] D. Moss, H. M. van Driel, and J. E. Sipe, "Dispersion in the anisotropy of optical third-harmonic generation in silicon," *Opt. Lett.*, vol. 14, no. 1, pp. 57–59, 1989.
[27] R. Claps, V. Raghunathan, D. Dimitropoulos, and B. Jalali, "Influence of nonlinear absorption on raman amplification in silicon waveguides," *Opt. Exp.*, vol. 12, no. 12, pp. 2774–2780, 2004.
[28] X. Chen and H. K. Tsang, "Nanoholes grating couplers for coupling between silicon-on-insulator waveguides and optical fibers," *IEEE Photon. J.*, vol. 1, no. 3, pp. 184–190, 2009.
[29] Y. Ding, H. Ou, and C. Peucheret, "Ultrahigh-efficiency apodized grating coupler using fully etched photonic crystals," *Opt. Lett.*, vol. 38, no. 15, pp. 2732–2734, Sep. 2013.